

Original Research

Core Ideas

- The CDE predicts non-physical dispersive solute flux against water flow direction.
- This wrongly directed dispersive solute flux can be as high as the convective flux.
- This problem occurs around zones with an increase or decrease in concentration.
- Particular cases are vaporization of water, root water uptake, and biodegradation.

Division of Soil Science and Soil Physics, Inst. of Geocology, Technische Univ. Braunschweig, Braunschweig, Germany. *Corresponding author (a.peters@tu-braunschweig.de).

Received 26 June 2019.
Accepted 23 Aug. 2019.

Citation: Peters, A., S.C. Iden, and W. Durner. 2019. Local solute sinks and sources cause erroneous dispersion fluxes in transport simulations with the convection–dispersion equation. *Vadose Zone J.* 18:190064. doi:10.2136/vzj2019.06.0064

© 2019 The Author(s). This is an open access article distributed under the CC BY-NC-ND license (<http://creativecommons.org/licenses/by-nc-nd/4.0/>).

Local Solute Sinks and Sources Cause Erroneous Dispersion Fluxes in Transport Simulations with the Convection–Dispersion Equation

Andre Peters,* Sascha C. Iden, and Wolfgang Durner

The convection–dispersion equation (CDE) is the most widely used model for simulating the transport of dissolved substances in porous media. The dispersion term in the CDE lumps molecular diffusion and hydromechanical dispersion into an effective diffusive solute flux. This is possible by describing hydrodynamic dispersion with Fick's first law of diffusion. We critically analyzed this concept for specific water flow situations where the solute concentration is locally increased by processes like root water uptake or water evaporation. The local accumulation of solutes in these situations leads to high concentration gradients and a dispersive solute flux component opposite to the direction of the water flux. This is physically wrong because it assumes that molecules or ions are moving against the flow direction by dispersion. The aim of this study was to investigate the magnitude of the resulting error by means of numerical modeling. We simulated solute transport from a groundwater table to a bare soil surface during steady-state evaporation using the HYDRUS-1D code. The simulations showed that in the region where dissolved substances accumulate due to the transition from liquid water to vapor, the resulting incorrect dispersive flux against the mean transport direction can reach the same order of magnitude as the convective solute flux. Under such conditions, application of the CDE is questionable.

Abbreviations: CDE, convection–dispersion equation; PDI, Peters–Durner–Iden.

Macroscopic modeling of solute transport in porous media is usually done with the convection–dispersion equation (CDE) (Vanclooster et al., 2006). The CDE is frequently applied at a large variety of scales, ranging from the centimeter scale in packed laboratory columns to the kilometer scale for problems of solute transport in groundwater (Hunt et al., 2011). The mathematical derivation of the CDE distinguishes three solute transport processes: (i) convection due to macroscopic transport of the solute with the mean velocity of the liquid phase; (ii) diffusion due to random movement of the single molecules within the liquid phase (molecular diffusion); and (iii) hydrodynamic dispersion due to uneven velocity in the flow field (Bear, 1972). The latter can be attributed to three causes: (i) variation of the flow velocity within single pores leads to the highest transport velocity at the center and zero velocity at the pore walls; (ii) pores of different size have different mean flow velocities; and (iii) solute molecules and ions have different path lengths on their tortuous flow path in the porous medium (Bear, 1972). Since dispersion is eventually caused by micro-convection, its extent depends on flow velocity, and there is no dispersion if water does not move. Due to diffusion, the single molecules will move randomly through the flow field of the moving liquid and thus “experience” different flow velocities (Flühler et al., 1996). According to the central limit theorem (Scheidegger, 1954), this will lead to a macroscopic spreading of concentration peaks toward a Gaussian distribution if the transport distance is sufficiently long. Therefore, dispersion is usually described with the same mathematical model as molecular diffusion and both processes are lumped together into an effective diffusion–dispersion coefficient (Jury and Horton, 2004, p. 228).

The dispersive solute flux depends on the solute concentration gradient and the flow velocity. In general, the hydrodynamic dispersion coefficient, D_{disp} ($\text{cm}^2 \text{d}^{-1}$) can be formulated as a function of the mean flow velocity by $D_{\text{disp}} = \lambda v^b$ (Biggar and Nielsen, 1976), with λ (cm) being the so-called dispersivity or dispersion length, v (cm d^{-1}) being the

mean water flow velocity, and b (dimensionless) being an empirical coefficient. For simplicity, b is set to unity in almost all model formulations of the CDE. Because the dispersivity is determined by the geometry of the water-filled pore space, it is regarded as a material constant.

Describing the dispersion process as apparent diffusion has been justified in many investigations of solute transport (Vanderborght and Vereecken, 2007). Because it is just an approximation of the real transport process, it is well known that the applicability of the concept is restricted to situations where the transport distance is large enough with respect to the dispersion length so that the central limit theorem is applicable (Bhattacharya and Gupta, 1983).

Several studies have been conducted that question the general usability of the CDE for solute transport in porous media (see, e.g., Cortis and Berkowitz [2004] and the literature cited therein). One critique is directed toward the fact that the dispersivity, which is assumed to be a material constant, is in fact highly scale dependent (e.g., Silliman and Simpson, 1987; Gelhar et al., 1992; Vanderborght and Vereecken, 2007). In their review of dispersivities in groundwater systems, Gelhar et al. (1992) derived as a rule of thumb that the dispersivity is approximately 10% of the transport distance. A similar result was found by Vanderborght and Vereecken (2007) for variably saturated soils. Another critique is that for heterogeneous and seemingly homogenous soil properties, an early and late arrival of solutes is sometimes observed, which cannot be described by Fick's law. This is often called "non-Fickian" transport (e.g., Levy and Berkowitz, 2003) and might be caused by preferential flow. Solutions for this problem are, e.g., using (i) the mobile-immobile concept (van Genuchten and Wierenga, 1976), (ii) the dual permeability concept (Gerke and van Genuchten, 1993), (iii) ensemble-averaged CDE or stochastic perturbation approaches (see Dagan and Neuman, 1997), or (iv) random walk particle tracking approaches (e.g., Cortis and Berkowitz, 2004). Column experimental studies with unsaturated porous media revealed that the dispersion length might also depend on water content (e.g., De Smedt and Wierenga, 1984; Toride et al., 2003). A solution is to account for this dependency in the model (Toride et al., 2003). However, due to its simplicity and the availability of analytical solutions for simple cases, the CDE is widely used to predict solute movement in saturated as well as variably saturated porous media. We like to stress that in all the above-mentioned solutions, except for some special cases of random walk particle tracking in which non-Gaussian perturbances are used, there is always a dispersion term that is formulated in the same mathematical way as molecular diffusion.

In this study, we focused on the following fundamental difference between diffusion and dispersion: Dispersive flux is caused by the fact that ions and molecules are moving faster or slower than the mean flow velocity due to uneven velocity in the flow field, but the molecules will never move against the macroscopic flow direction by dispersion. In contrast, diffusion leads to transport along and opposite to the macroscopic flow direction. Under certain

conditions, this difference can lead to fundamental inconsistencies when using the CDE for solute transport simulations. Examples of that are (i) a local increase in solute concentration due to vaporization of liquid water at or below the soil surface or due to root water uptake with solute exclusion and (ii) a local decrease in the liquid solute concentration due to decomposition of organic solutes. The latter might also lead to a local increase in the reaction product (metabolite), which subsequently undergoes solute transport.

Figure 1 schematically illustrates the two basic cases discussed above. Consider an initially homogeneous concentration (black dashed line) with the macroscopic water flux directed upward. If there is a local increase in the concentration (yellow line), diffusion and dispersion will lead to a matter flux from the solute peak toward the surrounding depths with lower concentrations. The induced calculated dispersive flux, which is directed opposite to the main water flow direction (in this case downward) is physically wrong because it assumes that molecules are flowing against the flow direction. Similarly, if there is a local sink (blue line), diffusion and dispersion will be directed from the surrounding toward the lowest concentration. Again, a dispersive flow against the main water flow direction will be predicted.

Fujimaki et al. (2006) conducted evaporation experiments with soil columns and allowed salt accumulation at the surface. They showed that the use of the CDE to simulate these experiments led to a wrong dispersion of the solute against the flow direction, which significantly delayed predicted salt accumulation at the soil surface. As a workaround, the dispersivities at the top 2 cm of the soil columns were reduced to better match the measured concentrations by the simulation. We note that although smaller dispersivities reduce the error of the transport model, the wrong dispersive flux against the flow direction remains.

The aim of this contribution was to critically analyze the CDE with respect to its inconsistency for modeling solute transport in

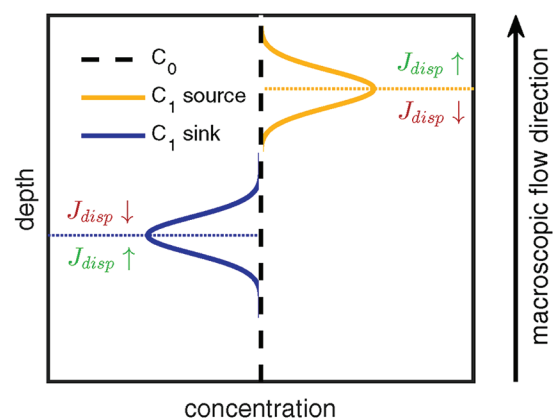


Fig. 1. Schematic illustration of the problems resulting from describing hydrodynamic dispersion with Fick's first law. Black dashed line: initially homogenous concentration; yellow line: a solute source leads to an increase in concentration at a certain depth; blue line: a solute sink leads to a decrease in the concentration at a certain depth. Yellow and blue dotted lines indicate locations of solute source and sink, respectively. The induced upstream dispersive flux (J_{disp}) (in this case downward and in red) is physically wrong.

variably saturated soils with local accumulation of solutes. We focus on the case of a local increase in concentration as an effect of the evaporation of water within the soil profile.

Theory

Modeling Water Flow

Coupled flow of liquid water (q_{liq} [cm d⁻¹]) and water vapor (q_{vap} [cm d⁻¹]) was simulated using the HYDRUS-1D code (Šimůnek et al., 2013). The soil hydraulic properties, i.e., the soil water retention function $\theta(h)$ and the hydraulic conductivity function $K(h)$, where θ (dimensionless) is the volumetric liquid water content, h (cm) is pressure head, and K (cm d⁻¹) is the liquid hydraulic conductivity, were described with the Peters–Durner–Iden (PDI) model (see Peters, 2013, 2014; Iden and Durner, 2014). In contrast to classic models of the soil hydraulic properties like the models of van Genuchten–Mualem (van Genuchten, 1980; Mualem, 1976), the PDI models assume liquid water retention and flow in capillaries and films and edges. In the dry range, water content decreases linearly on the semi-logarithmic scale toward zero at $\text{pF} = 6.8$ [$\text{pF} = \log_{10}(-h \text{ [cm]})$], which corresponds to oven dryness. For details, see the original papers.

Isothermal vapor flow is modeled in HYDRUS-1D as described by Saito et al. (2006). Phase transition from the liquid (θ) to the vapor phase (θ_{vap}) and vice versa is modeled under the assumption that both phases are in instantaneous local equilibrium. The underlying theory and the equations for calculating the fluxes of liquid water and water vapor are given in Nassar and Horton (1992).

The simulations in this study were performed for a coarse sand. Retention and conductivity data of a soil sample have been determined with the evaporation method, as described by Peters et al. (2015). The soil hydraulic functions and the isothermal vapor conductivity function are shown in Fig. 2. The hydraulic functions were obtained by fitting the PDI model, with the van Genuchten (1980) function representing the capillary water fraction, to the measured data using weighted least squares regression.

We simulated water flow from a static groundwater table located at two different depths ($L = 150$ and 300 cm) to a bare soil surface with constant atmospheric demand. At the lower boundary ($z = L$), a Dirichlet boundary condition with pressure

head $h = 0$ was used. The upper boundary was a system-dependent boundary with a prescribed flux density of 1 cm d^{-1} . This flux was maintained until the pressure head at the top boundary reached a pF of 6. This value corresponds to a relative humidity of 48% at a temperature of 20°C . When this value was reached, the boundary condition was switched to a Dirichlet condition with $\text{pF} = 6$. The initial condition was set to a hydrostatic pressure head distribution with $h = 0$ at the bottom. The simulation was continued until steady-state conditions were reached, as indicated by time-invariant water contents, pressure heads, and fluxes in the profile. We assumed steady-state conditions when the bottom and top flux densities did not change anymore within the numerical resolution of HYDRUS-1D. Although water flow under steady-state conditions can be modeled with an ordinary differential equation (Peters, 2013), we used the HYDRUS-1D software package because of its user-friendly interface, flexibility, and the fact that it has been verified many times. We discretized the domain into 500 equidistant finite elements.

Modeling Solute Transport

After the water flow simulation had reached steady state, the transport of a conservative solute undergoing no chemical reactions was simulated. We assumed that the solute originated from the groundwater and was transported with the liquid water phase upward toward the bare soil surface. One-dimensional transport of a nonreactive solute without sinks and sources was modeled with the CDE as implemented in HYDRUS-1D:

$$\frac{\partial(\theta C)}{\partial t} = -\frac{\partial}{\partial z}(J_{\text{conv}} + J_{\text{diff}} + J_{\text{disp}}) \quad [1]$$

where J_{conv} (mmol cm⁻² d⁻¹), J_{diff} (mmol cm⁻² d⁻¹), and J_{disp} (mmol cm⁻² d⁻¹) are convective, diffusive, and dispersive fluxes, respectively, given by

$$J_{\text{conv}} = v\theta C \quad [2]$$

$$J_{\text{diff}} = -D_{\text{diff}}\theta \frac{\partial C}{\partial z} \quad [3]$$

$$J_{\text{disp}} = -D_{\text{disp}}\theta \frac{\partial C}{\partial z} \quad [4]$$

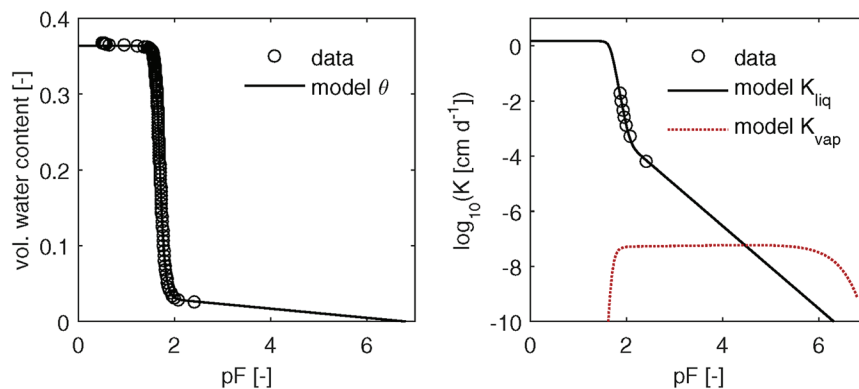


Fig. 2. Hydraulic functions for the coarse sand used in the simulations: soil water retention function, i.e., volumetric water content (θ) as a function of pF [$\text{pF} = \log_{10}(-h \text{ [cm]})$] (left), and hydraulic conductivity function, i.e., hydraulic conductivity (K) as a function of pF (right); K_{liq} , conductivity for the liquid phase; K_{vap} , conductivity for the vapor phase. The data points were determined with the evaporation method. The lines denote the fitted hydraulic functions (Peters–Durner–Iden model).

with

$$D_{\text{diff}} = \xi(\theta) D_1^w \quad [5]$$

$$D_{\text{disp}} = \lambda v \quad [6]$$

where C (mmol cm^{-3}) is the liquid-phase concentration, v (cm d^{-1}) is the mean pore water velocity, t (d) is time, z (cm) is the spatial coordinate, D_1^w ($\text{cm}^2 \text{d}^{-1}$) is the diffusion coefficient of the solute in pure water, ξ (dimensionless) is the tortuosity coefficient, and λ (cm) is longitudinal dispersivity. The mean pore water velocity is defined as $v = q_{\text{liq}}/\theta$ with the flux density of liquid water q_{liq} (cm d^{-1}). The tortuosity coefficient was parameterized with the Millington and Quirk (1961) model: $\xi = \theta^{7/3}/\theta_s^2$; D_{diff} ($\text{m}^2 \text{d}^{-1}$) and D_{disp} ($\text{m}^2 \text{d}^{-1}$) are the diffusion and hydrodynamic dispersion coefficients, respectively.

At the lower boundary ($z = L$), a Dirichlet condition was set with a constant concentration, $C_L = 0.1 \text{ mmol cm}^{-3}$, mimicking a well-mixed groundwater reservoir. At the upper boundary, a no-flux concentration was applied, reflecting the fact that the non-reactive solute can neither flow nor volatilize across the soil surface. The soil profile was initially assumed to be solute free. Since the solute is transported in a profile that is initially free of solute from the bottom, any simulated dispersion against the flow direction is caused by a local increase in concentration. This implies that ions or molecules that have accumulated there are transported against the flow direction by dispersion, which is physically wrong.

Dispersivities were set to $0.1L$, $0.01L$, and $0.001L$. For simplicity, D_1^w was set to $1 \text{ cm}^2 \text{d}^{-1}$, which roughly corresponds to the average value of major ions at 25°C reported by Appelo and Postma (2005). The simulation time was chosen to ensure that the maximum concentration C in the profile did not exceed the saturation concentration of a typical salt, i.e., NaCl, which is around 6.1 mmol cm^{-3} at 25°C . The discretization of 500 equidistant elements guaranteed that the grid Peclet number was always ≤ 2 to ensure numerical stability. The Crank–Nicholson and upstream weighing schemes were applied for time and space weighing.

We note that the underlying assumption for this study might not be entirely fulfilled in real systems. Salt accumulation would, for example, continuously decrease the osmotic potential and thus the water potential in the soil. This would lead to a decrease of the evaporation rate (Fujimaki et al., 2006) and would add another driving force for water flow. Finally, the times required to establish steady-state conditions are between $\approx 1000 \text{ d}$ ($L = 150 \text{ cm}$) and $\approx 10,000 \text{ d}$ ($L = 300 \text{ cm}$).

Results and Discussion

Steady-State Water Flow

Figure 3 shows the depth distribution of the volumetric water content, liquid and vapor water flux densities, and mean pore water velocity of the simulation for the profile with depth $L = 150 \text{ cm}$. The water content decreases with height, with a sharp decrease at a depth of about 25 cm above which vapor flow exceeds liquid water flow (Fig. 3, center). The mean pore water velocity v increases as water content decreases, reaching its maximum just below the depth where vapor transport becomes dominant (Fig. 3, right). Above that depth, v sharply decreases again. An accumulation of a nonvolatile solute is expected at exactly this depth because it is not transported in the gas phase. Note that the water content at the top does not reach zero but a low finite value (≈ 0.005). This is in accordance with the formulation of the PDI water retention function, where the water content becomes zero only at a pressure head of $-10^{6.8} \text{ cm}$ (Fig. 2, left), whereas the pressure head at the top is $-10^{6.0} \text{ cm}$. As a consequence, also the mean pore water velocity becomes small but not zero at the top.

Solute Transport

The depth distributions of D_{diff} and D_{disp} (Eq. [5] and [6]) for the profile with length $L = 150 \text{ cm}$ are shown in Fig. 4. Due to the small water flow velocity, D_{disp} is small for all values of λ at the bottom. However, closer to the surface v sharply increases (Fig. 3) and so does D_{disp} , whereas water content and thus D_{diff} decrease (note the logarithmic scale of the abscissa). At the depth where the solute accumulation is expected ($z \approx 25 \text{ cm}$), D_{disp} is at least one order of magnitude higher than D_{diff} . We note that the predictive model of Millington and Quirk (1961), which is the standard model to predict the tortuosity coefficient for solute transport in unsaturated porous media, seems to underestimate D_{diff} for low water contents, since values measured by Tokunaga et al. (2017) are about one to two orders of magnitude higher than our calculated values. However, D_{disp} is in most cases much higher than D_{diff} at the depth of solute accumulation. Therefore, we discuss only the dispersive fluxes in the following.

Figure 5 shows the depth distributions of the simulated solute concentration for the different dispersivities at three different times. Since the solute is transported only in the liquid phase and liquid water flux decreases sharply at a depth of approximately 25 cm, the solute accumulates at this depth. As

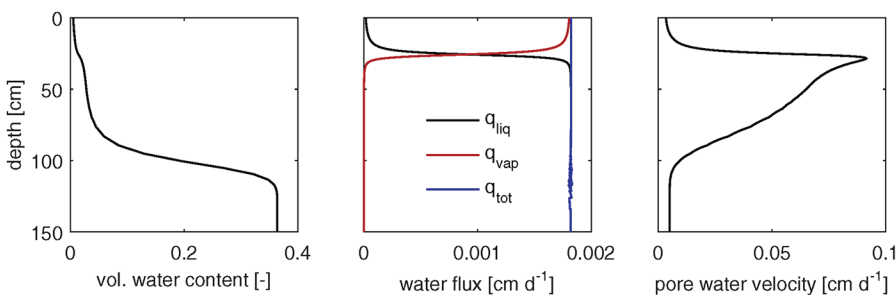


Fig. 3. Depth distribution of volumetric water content (left), depth distribution of liquid (q_{liq}), vapor (q_{vap}), and total water flux density (q_{tot}) (center), and depth distribution of the average pore water velocity (v) (right).

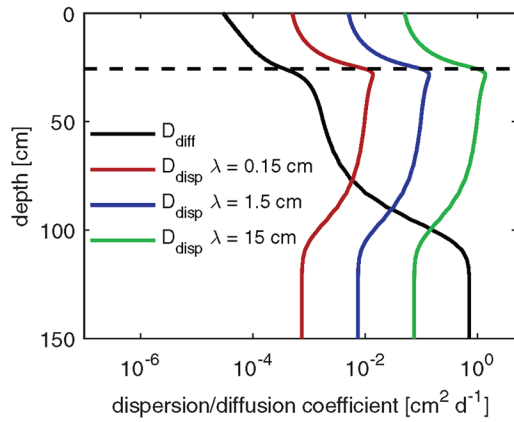


Fig. 4. Depth distribution of the dispersion coefficient D_{disp} , with three different dispersion lengths λ , and the diffusion coefficient D_{diff} . At the depth of interest (approximately 25 cm), D_{disp} is at least one order of magnitude higher than D_{diff} for all dispersivities. The dashed line indicates the depth at which vapor and liquid flow are equal; above this level, vapor flow is dominant (see Fig. 3).

expected, this increase in concentration is higher for small values of λ . Note that only dispersion plays a role for solute spreading in our modeling study, since $D_{\text{disp}} \gg D_{\text{diff}}$ for all depths down to ≈ 80 cm (Fig. 4).

Although the vapor flux exceeds the liquid water flux in the top centimeters, there is still a small liquid flux and a water

content greater than zero. Thus the solute is slowly transported toward the top, where it eventually accumulates because of the no-flux condition at the top. This process is faster for higher dispersivities.

The depth distributions of the convective (J_{conv}) and dispersive (J_{disp}) solute fluxes are shown in Fig. 6. Positive fluxes are directed upward and negative fluxes directed downward. As expected, the convective flux is always directed upward, whereas the dispersive flux is directed downward (upstream) and upward (downstream). The same holds for the flux caused by molecular diffusion, which is not shown because it is at least one order of magnitude smaller than the dispersive flux in all cases. While the upstream (i.e., downward) diffusive flux is physically correct because it is caused by random motion, the upstream dispersive flux, which is caused by the local accumulation of the solute around $z = 25$ cm, is in this case clearly unphysical. In the case $\lambda = 15$ cm (1/10 of the column length), the dispersive flux even reaches the magnitude of the convective flux. This illustrates that the error due to CDE-modeled upstream dispersion caused by a local increase of concentrations can be remarkably high. The results for the soil depth of 300 cm look similar and therefore confirm these findings (Fig. 7). For shorter columns, the evaporation plane is located near the surface but the results show again that the upstream dispersion has the same magnitude as convection for $\lambda = 0.1L$ (not shown).

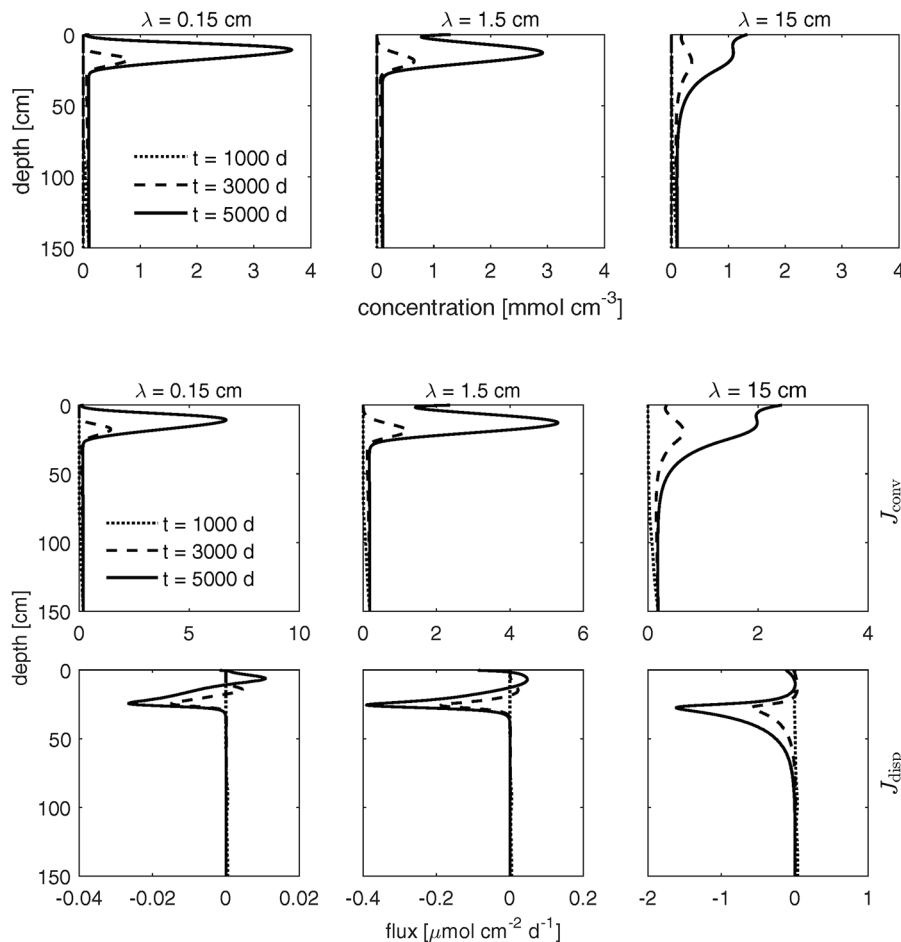


Fig. 5. Solute concentration profiles at three times for three values of the dispersion length λ . Note that at time $t = 1000$ d (dotted line), the concentration is low in the whole profile and the solute has not yet been transported to the enrichment depth at 25 cm.

Fig. 6. Depth distribution of convective (top) and dispersive (bottom) fluxes (J_{conv} and J_{disp} , respectively) at three different times t for three different values of the dispersion length λ . The profile depth is 150 cm.

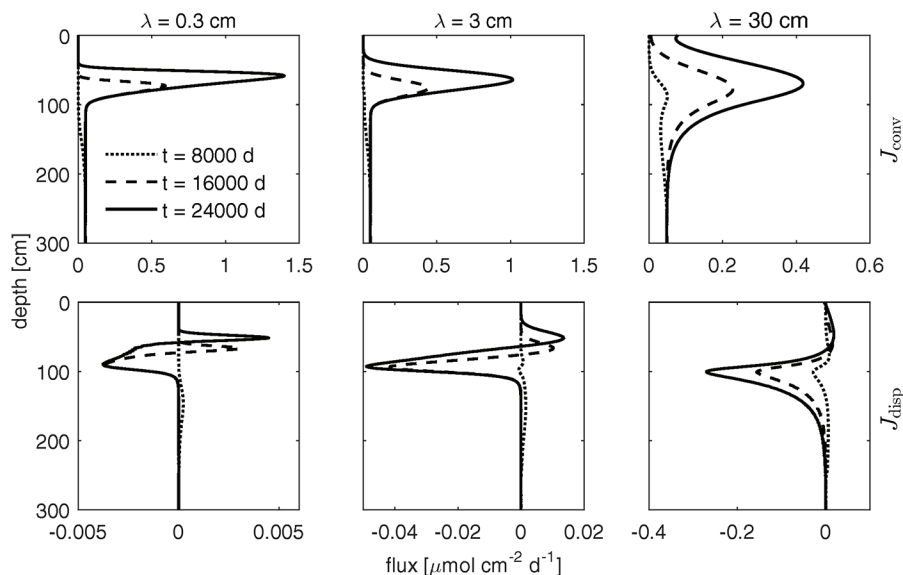


Fig. 7. Depth distribution of convective (top) and dispersive (bottom) fluxes (J_{conv} and J_{disp} , respectively) at three different times t for three different values of the dispersion length λ . The profile depth is 300 cm.

Conclusions

Our study shows that describing the hydrodynamic dispersion process of solutes in variably saturated porous media by Fick's first law can lead, under specific flow and transport conditions, to an implausible direction and magnitude of the dispersive flux and therefore to wrong simulation results. Specifically, if the solute concentration in the transporting liquid increases locally by processes like vaporization of the liquid water (treated in this work) or root water uptake with solute exclusion, or decreases locally by processes like precipitation or local decay, the description of hydrodynamic dispersion by Fick's law leads to solute flux predictions that are wrong. This holds for the classic CDE, extensions thereof, e.g., the mobile-immobile dual-porosity transport model, and also for specific random-walk particle tracking models where macroscopic dispersion is described as an isotropic random transport process. If the CDE is used under such conditions, the error associated with a simulation should be approximately quantified or estimated. If the error is too large, an alternative model needs to be taken into account. At this stage we are not able to give well-founded general advice concerning at what point the error is too large, but the error is obvious if the dispersive flux component reaches the same magnitude as the advective component. Suitable alternative models under such conditions might be random-walk particle tracking methods in which dispersion is implemented as an anisotropic random process or a numerical solution of the two- or three-dimensional Navier–Stokes equation for water flow and a subsequent numerical solution of the two- or three-dimensional convection–diffusion equation for the resulting water flow field. Appropriate experimental studies are necessary to test and improve the different approaches.

References

- Appelo, C.A.J., and D. Postma. 2005. *Geochemistry, groundwater and pollution*. 2nd ed. Balkema, Leiden, the Netherlands.
- Bear, J. 1972. *Dynamics of fluids in porous media*. American Elsevier, New York.
- Bhattacharya, R.N.V.K., and V.K. Gupta. 1983. A theoretical explanation of solute dispersion in saturated porous media at the Darcy scale. *Water Resour. Res.* 19:938–944. doi:10.1029/WR019i004p00938
- Biggar, J.W., and D.R. Nielsen. 1976. Spatial variability of the leaching characteristics of a field soil. *Water Resour. Res.* 12:78–84. doi:10.1029/WR012i001p00078
- Cortis, A., and B. Berkowitz. 2004. Anomalous transport in “classical” soil and sand columns. *Soil Sci. Soc. Am. J.* 68:1539–1548. doi:10.2136/sssaj2004.1539
- Dagan, G., and S.P. Neuman, editors. 1997. *Subsurface flow and transport: A stochastic approach*. Cambridge Univ. Press, New York. doi:10.1017/CBO9780511600081
- De Smedt, F., and P.J. Wierenga. 1984. Solute transfer through columns of glass beads. *Water Resour. Res.* 20:225–232. doi:10.1029/WR020i002p00225
- Flühler, H., W. Durner, and M. Flury. 1996. Lateral solute mixing processes: A key for understanding field-scale transport of water and solutes. *Geoderma* 70:165–183. doi:10.1016/0016-7061(95)00079-8
- Fujimaki, H., T. Shimano, M. Inoue, and K. Nakane. 2006. Effect of a salt crust on evaporation from a bare saline soil. *Vadose Zone J.* 5:1246–1256. doi:10.2136/vzj2005.0144
- Gelhar, L.W., C. Welty, and K.R. Rehfeldt. 1992. A critical review of data on field-scale dispersion in aquifers. *Water Resour. Res.* 28:1955–1974. doi:10.1029/92WR00607
- Gerke, H.H., and M.Th. van Genuchten. 1993. A dual-porosity model for simulating the preferential movement of water and solutes in structured porous media. *Water Resour. Res.* 29:305–319. doi:10.1029/92WR02339
- Hunt, A.G., T.E. Skinner, R.P. Ewing, and B. Ghanbarian-Alavijeh. 2011. Dispersion of solutes in porous media. *Eur. Phys. J. B* 80:411–432. doi:10.1140/epjb/e2011-10805-y
- Iden, S.C., and W. Durner. 2014. Comment on “Simple consistent models for water retention and hydraulic conductivity in the complete moisture range” by A. Peters. *Water Resour. Res.* 50:7530–7534. doi:10.1002/2014WR015937
- Jury, W.A., and R. Horton. 2004. *Soil physics*. 6th ed. John Wiley & Sons, New York.
- Levy, M., and B. Berkowitz. 2003. Measurement and analysis of non-Fickian dispersion in heterogeneous porous media. *J. Contam. Hydrol.* 64:203–226. doi:10.1016/S0169-7722(02)00204-8
- Millington, R.J., and J.M. Quirk. 1961. Permeability of porous solids. *Trans. Faraday Soc.* 57:1200–1207. doi:10.1039/tf9615701200
- Mualem, Y. 1976. A new model for predicting the hydraulic conductivity of unsaturated porous media. *Water Resour. Res.* 12:513–522. doi:10.1029/WR012i003p00513

- Nassar, I.N., and R. Horton. 1992. Simultaneous transfer of heat, water, and solute in porous media: I. Theoretical development. *Soil Sci. Soc. Am. J.* 56:1350–1356. doi:10.2136/sssaj1992.03615995005600050004x
- Peters, A. 2013. Simple consistent models for water retention and hydraulic conductivity in the complete moisture range. *Water Resour. Res.* 49:6765–6780. doi:10.1002/wrcr.20548
- Peters, A. 2014. Reply to comment by S. Iden and W. Durner on “Simple consistent models for water retention and hydraulic conductivity in the complete moisture range.” *Water Resour. Res.* 50:7535–7539. doi:10.1002/2014WR016107
- Peters, A., S.C. Iden, and W. Durner. 2015. Revisiting the simplified evaporation method: Identification of hydraulic functions considering vapor, film and corner flow. *J. Hydrol.* 527:531–542. doi:10.1016/j.jhydrol.2015.05.020
- Saito, H., J. Šimůnek, and B. Mohanty. 2006. Numerical analyses of coupled water, vapor, and heat transport in the vadose zone. *Vadose Zone J.* 5:784–800. doi:10.2136/vzj2006.0007
- Scheidegger, A.E. 1954. Statistical hydrodynamics in porous media. *J. Appl. Phys.* 25:994–1001. doi:10.1063/1.1721815
- Silliman, S.E., and E.S. Simpson. 1987. Laboratory evidence of the scale effect in dispersion of solutes in porous media. *Water Resour. Res.* 23:1667–1673. doi:10.1029/WR023i008p01667
- Šimůnek, J., M. Šejna, H. Saito, M. Sakai, and M.Th. van Genuchten. 2013. The HYDRUS-1D software package for simulating the movement of water, heat, and multiple solutes in variably saturated media. Version 4.17. Dep. of Environ. Sci., Univ. of California, Riverside.
- Tokunaga, T.K., S. Finsterle, Y. Kim, J. Wan, A. Lanzirotti, and M. Newville. 2017. Ion diffusion within water films in unsaturated porous media. *Environ. Sci. Technol.* 51:4338–4346. doi:10.1021/acs.est.6b05891
- Toride, N., M. Inoue, and F.J. Leij. 2003. Hydrodynamic dispersion in an unsaturated dune sand. *Soil Sci. Soc. Am. J.* 67:703–712. doi:10.2136/sssaj2003.0703
- Vanclooster, M., M. Javaux, and J. Vanderborght. 2006. Solute transport in soil at the core and field scale. In: M.G. Anderson, editor, *Encyclopedia of hydrological sciences*. Vol. 2. John Wiley & Sons, New York. p. 1041–1055. doi:10.1002/0470848944.hsa073
- Vanderborght, J., and H. Vereecken. 2007. Review of dispersivities for transport modeling in soils. *Vadose Zone J.* 6:29–52. doi:10.2136/vzj2006.0096
- van Genuchten, M.Th. 1980. Closed-form equation for predicting the hydraulic conductivity of unsaturated soils. *Soil Sci. Soc. Am. J.* 44:892–898. doi:10.2136/sssaj1980.03615995004400050002x
- van Genuchten, M.Th., and P.J. Wierenga. 1976. Mass transfer studies in sorbing porous media: I. Analytical solutions. *Soil Sci. Soc. Am. J.* 40:473–481. doi:10.2136/sssaj1976.03615995004000040011x